

# Augmented Marker Tracking for Peri-acetabular Osteotomy Surgery

Silvio Pflugi, Rakesh Vasireddy, Till Lerch, Timo M. Ecker, Moritz Tannast, Nane Boemke,  
Klaus Siebenrock and Guoyan Zheng

**Abstract**—We developed and validated a small, easy to use and cost-effective augmented marker-based hybrid navigation system for peri-acetabular osteotomy (PAO) surgery.

The hybrid system consists of a tracking unit directly placed on the patient's pelvis, an augmented marker with an integrated inertial measurement unit (IMU) attached to the patient's acetabular fragment and the host computer. The tracking unit sends a live video stream of the marker to the host computer where the marker's pose is estimated. The augmented marker with the IMU sends its pose estimate to the host computer where we apply sensor fusion to compute the final marker pose estimate. The host computer then tracks the orientation of the acetabular fragment during peri-acetabular osteotomy surgery. Anatomy registration is done using a previously developed registration device. A Kalman filter-based sensor fusion was added to complete the system. A plastic bone study was performed for validation between an optical tracking-based navigation system and our proposed system.

Mean absolute difference for inclination and anteversion was 1.63 degrees and 1.55 degrees, respectively. The results show that our system is able to accurately measure the orientation of the acetabular fragment.

## I. INTRODUCTION

Peri-acetabular osteotomy (PAO) surgery is commonly used for the treatment of adult hip dysplasia [6]. It is a demanding, open surgery where the surgeon separates the acetabular fragment from the rest of the pelvis before the fragment is reoriented to improve femoral head coverage. Many surgical navigation systems exist that support the surgeon during a PAO surgery. However, the current gold standard is still based on optical tracking. Dynamic Reference Bases (DRBs, active or passive) are attached to the patient's pelvis and fragment and are tracked by a large stereo camera [7], [11], [12]. Although optical tracking generally offers a very high accuracy, its main limitation is the line-of-sight impediment that is inherent with camera-only-based navigation systems. Additionally, such optical tracking-based systems need a lot of space in the operating room, limiting the space for the surgeon during the procedure. Alternative tracking techniques were proposed to overcome these drawbacks. One of them is electro-magnetic (EM) tracking which is able to track a small coil even inside the patient's body [8], [22]. It does not suffer from the line-of-sight impediment but is susceptible to magnetic field distortions. Recent advancements in microelectromechanical systems (MEMS) allowed the development of small and relatively cost-effective inertial measurement unit (IMU) based systems. IMUs generally combine two or more types of sensors into one small unit. A sensor fusion algorithm such as the well-known Kalman filter [9] is used to fuse

the information from all individual sensors. IMUs were previously used in the field of surgical navigation [1], [15], [20], [17]. Generally, IMUs use the accelerometer to define the "down" vector, the magnetometer to define the heading angle and the gyroscopes to drive the system dynamics that provides a prediction of the orientation. Similar to EM-based navigation systems, IMUs that include magnetometer sensors are sensitive to distorted magnetic field environments that are generally observable in an operating room (OR). Another problem with IMUs is the drift, stemming from the necessary integration of the gyroscope [1], [15]. Hybrid navigation systems, merging two or more technologies to overcome each individual technology's drawbacks, were proposed [5], [2], [3], [13]. Such hybrid systems offer high accuracy but are generally very complex and expensive. In this work, we propose a new hybrid system, combining an IMU with planar marker tracking known from augmented reality applications [4]. We combine a planar Aruco marker [4] with a low-cost IMU into one augmented marker which is attached to the patient's acetabular fragment. This marker is then tracked by a tracking unit which is directly placed on the patient's pelvis. The contribution of this work is the removal of the line-of-sight impediment by fusing the information from planar marker tracking with the orientation output from the IMU. The augmented marker also enables a convenient way for patient registration, based on our previously proposed technique [17], as it does not need to be in the field-of-view (FOV) of the tracking unit. The paper is divided into two parts: we first introduce the system components and the basic setup and procedure for PAO navigation. The second part covers our approach to sensor fusion including a plastic bone study for validation.

## II. MATERIAL AND METHODS

### A. System Overview

The system consists of three parts: 1) The tracking unit which consists of a miniature computer and a camera module that sends a live video stream over a wireless (WiFi) connection to the host computer. The tracking unit is placed on the patient's pelvis facing towards the acetabular fragment area. 2) An augmented marker consisting of a planar Aruco marker [4] with an integrated IMU (BNO055, Robert Bosch GmbH, Germany). The augmented marker is attached to the acetabular fragment in a way, that the planar marker faces the tracking unit and is inside the camera module's FOV. The IMU has built-in sensor fusion based on the signals from the gyroscopes and accelerometers. The orientation estimate from the IMU is sent to the host computer over a wireless

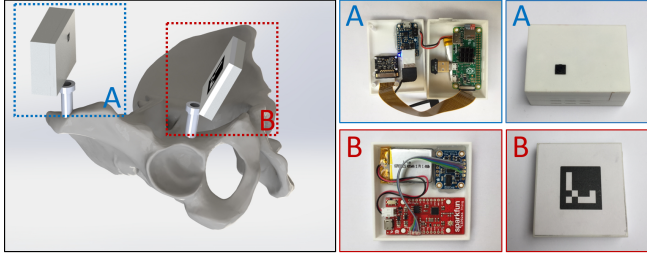


Fig. 1: A schematic illustration of how our system works. *Left:* The overall setup with the tracking unit (A) attached to the patient’s pelvis facing towards the acetabular fragment where the augmented marker is attached (B). *Middle:* Inside view at the two components. *Right:* Outside view at the two components.

(WiFi) connection. 3) The host computer receives the video stream from the tracking unit and the orientation estimates from the IMU. It is responsible for detecting the marker in the video stream and estimating the planar marker’s pose using a robust pose estimation algorithm [21]. Furthermore, sensor fusion is applied to compute a final pose estimate for the augmented marker. An overview of the system is shown in Figure 1.

### B. Conceptual Design

We previously proposed a PAO navigation system only relying on a monocular camera (attached to the patient’s pelvis) that tracks a planar marker attached to the patient’s acetabular fragment [18]. This setup significantly increases the available working space in the OR as no large camera setup is necessary. This system had the limitation that it was difficult to perform anatomy registration. We used a registration device which aligned the planar marker with the anterior pelvic plane (APP). This way, we were able to record the APP’s orientation and align the computer model with it to achieve patient registration. Compared to this previous work, we added an IMU to the planar marker design which now enables us, to record the orientation of the APP without the necessity of having the augmented marker in the FOV of the camera. In general, we can identify three challenges for navigated PAO surgery: 1) As we combine the IMU with a planar marker, it is necessary to first perform a calibration step to determine the transformation from the IMU local coordinate system to the planar marker’s local coordinate system. This has to be done only once. 2) Anatomy registration: since we only rely on rotational information, it is enough to estimate the orientation of the APP for patient registration. 3) Marker tracking during acetabular reorientation. The following sections will explain how we solved the three challenges in more detail.

### C. Calibration

The IMU is rigidly attached at the back of the planar marker. The goal of this calibration step is to estimate the fixed transformation between the IMU’s local coordinate system and the planar marker’s local coordinate system. This is a

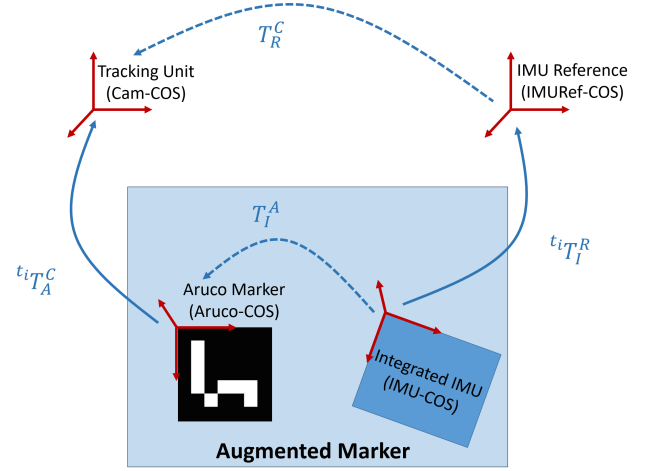


Fig. 2: A schematic illustration of the calibration of the transformation between the IMU and the planar Aruco marker.

typical hand-eye calibration problem [10], where we compute the unknown transformation using a set of measurements of the transformation of each local coordinate system with respect to its associated global coordinate system. We will first present the derivation of the problem and then give a solution based on Lie Group Theory [16]. The involved coordinate systems are shown in Figure 2. At any time  $t_i$ , we will receive two transformations from our tracking system, one is the transformation from the planar marker coordinate system (Aurco-COS) to the tracking unit’s camera coordinate system (Cam-COS) and the other is the transformation from the IMU coordinate system (IMU-COS) to its measurement reference space (IMURef-COS). Our aim is to compute the fixed transformation from the IMU-COS to the Aruco-COS. At two time points  $t_i$  and  $t_j$ , we have the following relationship:

$$T_I^A = {}^{t_i}T_C^A \cdot T_R^C \cdot {}^{t_i}T_I^R \quad (1)$$

and

$$T_I^A = {}^{t_j}T_C^A \cdot T_R^C \cdot {}^{t_j}T_I^R \quad (2)$$

With these two equations, we have two unknown transformations:  $T_I^A$  and  $T_R^C$ . We can eliminate  $T_R^C$  to obtain:

$$T_I^A = {}^{t_j}T_C^A \cdot ({}^{t_i}T_C^A)^{-1} \cdot T_I^A \cdot ({}^{t_i}T_I^R)^{-1} \cdot {}^{t_j}T_I^R \quad (3)$$

Let’s define

$${}^{t_{ij}}\Delta T_C^A = {}^{t_j}T_C^A \cdot ({}^{t_i}T_C^A)^{-1} \quad (4)$$

and

$${}^{t_{ij}}\Delta T_I^R = ({}^{t_j}T_I^R)^{-1} \cdot {}^{t_i}T_I^R \quad (5)$$

Then we have:

$$({}^{t_{ij}}\Delta T_C^A)^{-1} \cdot T_I^A = T_I^A \cdot {}^{t_{ij}}\Delta T_I^R \quad (6)$$

Without causing confusion, we arbitrarily select a time  $t_i = t_0$ , and the incremental transformations defined in equation 4 and 5 are measured with respect to this time point such that

we can drop the index  $i$ . Also, only considering the rotational part of the transformation, we end up with:

$$\Delta R_A^j \cdot R_I^A = R_I^A \cdot \Delta R_I^j \quad (7)$$

This is the classical equation of the form  $AX = XB$  known from hand-eye calibration literature [10], [16]. Following [16], we will use Lie group theory to convert the problem to a least-squares problem and derive a closed-form solution. More specifically, for a given rotation matrix  $R$ , we have:

$$\theta = \arccos\left(\frac{\text{trace}(R) - 1}{2}\right) \quad (8)$$

$$\log(R) = \begin{cases} 0, & \text{if } \theta = 0 \\ \text{skew}(r), & \text{if } \theta \neq 0 \text{ and } \theta \in (-\pi, \pi) \end{cases} \quad (9)$$

Where  $r = \theta a_R = [r_x r_y r_z]^T$  is the axis-angle representation of the rotation matrix  $R$  and:

$$\text{skew}(r) = \begin{bmatrix} 0 & -r_z & r_y \\ r_z & 0 & -r_x \\ -r_y & r_x & 0 \end{bmatrix}. \quad (10)$$

Applying this equation to  $\Delta R_I^j$ ,  $\Delta R_A^j$ , we have:

$$\log(\Delta R_A^j) = \text{skew}(b_j) \quad (11)$$

and

$$\log(\Delta R_I^j) = \text{skew}(a_j) \quad (12)$$

According to Lie theory, we have:

$$b_j = R_I^A a_j \quad (13)$$

In the presence of noise, we can formulate our original problem to the following least-squares minimization problem:

$$\min_{R_I^A} \sum_{j=1}^n |R_I^A a_j - b_j|^2 \quad (14)$$

Where a closed-form solution can be calculated efficiently as

$$R_I^A = U V^{-\frac{1}{2}} U^{-1} M^T \quad (15)$$

With  $M = \sum_{j=1}^n b_j a_j^T$ , and the eigen-decomposition of  $M^T M = U V U^{-1}$ .

#### D. Anatomy Registration

Anatomy registration is performed using our previously developed registration device [17] where three equal length pillars are placed on the three landmarks (left and right anterior superior iliac spine and one of the two pubic tubercles) defining the APP. To record the orientation of the APP, we take the augmented marker and put it on the top plate, aligning it with the APP. The FOV of the tracking unit's camera is very small so the Aruco marker is not visible during APP registration. Therefore, we perform the registration solely based on the measurements from the IMU. The augmented marker is fixed to the top plate in a way, that the local x-axis of the planar marker is aligned with the connection between the left and right superior iliac spines. This way, the local z-axis of the planar marker represents

the APP normal. Using the fixed calibration matrix, we can measure the orientation of the APP in the IMU reference coordinate system during APP registration. Right before the reorientation procedure starts, we will have both the tracking unit and the augmented marker attached to the patient (pelvis and acetabular fragment). At this moment, we can transform the recorded APP orientation from the IMU reference coordinate system to the IMU local coordinate system and further to the planar marker's local coordinate system using the fixed calibration matrix.

#### E. Tracking

The augmented marker is attached to the acetabular fragment in a way that the planar marker is in the tracking unit's FOV (see Figure 1). After the fragment is detached and right before the reorientation procedure is started, we record the initial orientation of the fragment at time  $t_0$ . During the reorientation procedure, at each time point  $t_i$ , we compute the difference in rotation to the previous time point and update the acetabular orientation accordingly. The reorientation is visualized on the host computer's screen. We compute radiographic anteversion and inclination angles according to [14].

#### F. Sensor Fusion

The host computer receives a video stream from the tracking unit and a stream of pose estimates from the IMU which is integrated into the augmented marker. An important step is to fuse the information coming from the IMU and tracking unit to compute a final pose estimate of the tracked augmented marker. As a reminder, the IMU used in this system already has built-in sensor fusion making use of the input from the gyroscopes and accelerometers. Our approach consists of two parts: during reorientation, we first start with a simple thresholding of the input video stream to detect the planar marker for the first time. In the next frame, we use the already fused output from the IMU to predict the location of the marker corner points in the next video frame. This allows us to restrict the search area in the image for the planar marker. With a smaller search area, it is possible to apply adaptive thresholding instead of using a fixed threshold for the whole image without decreasing the frame rate. In case that adaptive thresholding fails or if the marker goes outside the FOV of the camera, we simply fall back to a state, where we apply simple thresholding on the full image until the marker is detected again. On top of this marker tracking, we apply a simple Kalman filter [9], [19] where we use the input from the IMU as the prediction and the output from the marker tracking as the measurements for the correction part of the filter. During prediction, instead of using the previous state, we directly take the quaternion output from the IMU. A flowchart showing the steps of sensor fusion is shown in 4. The prediction equations of the Kalman filter are shown in Equation 16 and 17.

$$q_k = A_k q_k^{IMU} \quad (16)$$

$$P_{k|k-1} = A_k P_{k-1|k-1} A_k^T + Q_k \quad (17)$$

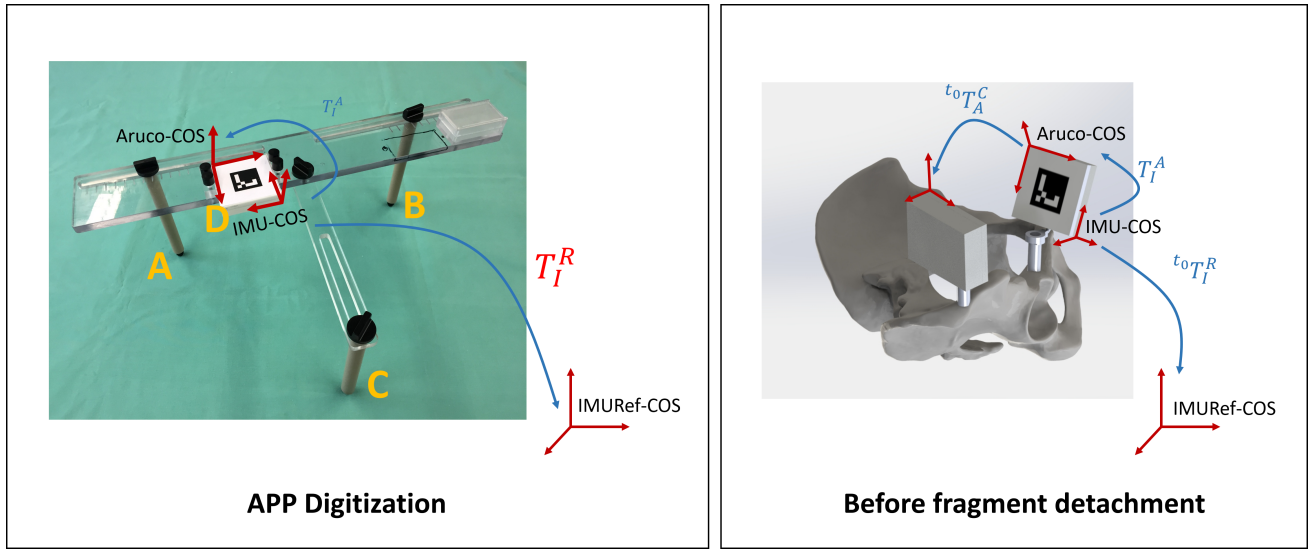


Fig. 3: A schematic representation of how anatomy registration is performed. *Left:* The previously developed registration device is designed in a way that the three equal-length pillars are placed on the patient's right (A) and left (B) superior iliac spine (ASIS) and on one pubic tubercle (C). This will align the planar marker's (D) x-axis with the connection between the two ASISs. The planar marker's local z-axis will then represent the anterior pelvic plane (APP) normal.  $T_I^A$  is the fixed calibration matrix.  $T_I^R$  is measured by the IMU. *Right:* The situation before the acetabular fragment is detached. We have all information available to bring the measured orientation for the APP into the planar marker's local coordinate system where we perform all computations during reorientation.

$A_k$  is the state transition matrix, set to identity,  $P_k$  is the state covariance matrix and  $Q_k$  is the process noise covariance matrix. The update equations are shown below:

$$y_k = q_k^{Marker} - H_k q_k \quad (18)$$

$$S_k = H_k P_{k|k-1} H_k^T + R_k \quad (19)$$

$$K_k = P_{k|k-1} H_k^T S_k^{-1} \quad (20)$$

$$q_k = q_k + K_k y_k \quad (21)$$

$$P_{k|k} = (I - K_k H_k) P_{k|k-1} \quad (22)$$

where  $y_k$  is the innovation,  $S_k$  the innovation covariance matrix,  $H_k$  the observation matrix (set to identity) and  $K_k$  is the Kalman gain. When marker detection fails, the filter does not perform an update step and instead, the final orientation output is the one after the prediction step.

#### G. Validation

A validation plastic bone study including 3 pelvises (6 hip joints) undergoing navigated PAO was performed. For comparison, we simultaneously ran a previously proposed and validated optical tracking-based navigation system [12] using an optical stereo-camera (Polaris, NDI, Canada). We reoriented the acetabular fragment to 20 random positions and simultaneously recorded inclination and anteversion from both systems. We performed all necessary steps (anatomy registration, fragment reorientations) for each hip joint ( $N = 120$  different reorientation positions).

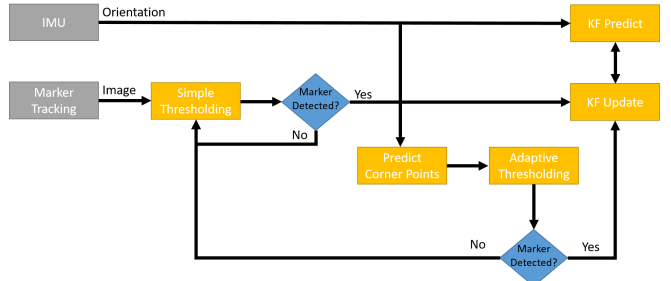


Fig. 4: Sensor fusion flow chart. The Kalman filter is initialized using the first pose estimate from marker tracking. After initialization, the prediction of the Kalman filter is the IMUs orientation output. If simple thresholding was successful, then we use the IMU orientation to predict the corner points of the marker in the next frame. The marker is then detected using adaptive thresholding in a smaller search area. If the marker is detected, we hand the pose estimate to the update step of the Kalman filter, if not, we go back to perform marker detection in the full input image using simple thresholding.

### III. RESULTS

Inclination and anteversion values measured by our system show a strong correlation to the ground-truth system (0.99 / 0.96). Figure 5 shows the median error and the 5-th and 95-th percentiles for each individual case. Mean absolute difference for inclination and anteversion ( $N = 120$ ) was 1.63 degrees and 1.55 degrees, respectively.

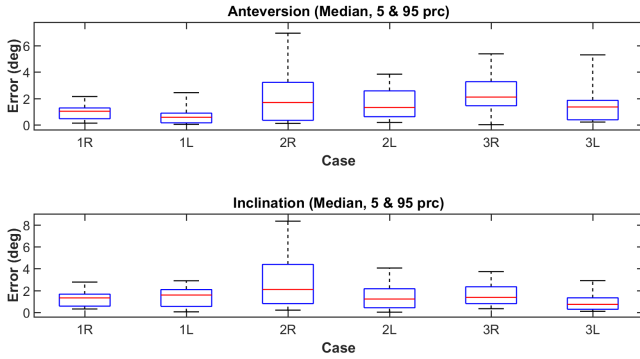


Fig. 5: Error box plot for anteversion (top) and inclination (bottom). The 5-th and 95-th percentiles and the median error (red line) are shown for each case. Letters L/R represent hip joint side for a specific hip joint.

#### IV. DISCUSSION

In this work we successfully demonstrated the feasibility of our system to measure the acetabular orientation during PAO reorientation procedure. We compared our hybrid navigation system to a previously developed and validated optical tracking-based system [12] which served as ground-truth.

Strong correlation and small mean differences for both anteversion and inclination were found compared to the ground-truth system. Our proposed system offers an easy setup, minimal space requirements and does not suffer from the line-of-sight impediment.

The tracking unit is directly placed on the patient's pelvis, which is very close to the surgical area. This is necessary for the small camera module to be able to accurately track the augmented marker. The tracking unit is placed on the pelvis after the acetabular fragment is separated from the pelvis. This procedure should prevent blood splatters on the camera lens as no further surgical actions must be performed when the tracking unit is running.

Another limitation is that we solely rely on the IMU during anatomy registration. This offers a higher convenience, as we are not limited by the line-of-sight to the tracking unit. IMUs offer a lower accuracy due to drift [1], [15]. This however, should not affect the outcome too much, as the time to perform the registration is very short (around 30-60s) which limits the error introduced by drift. In this study, we did not notice any larger error that can be explained by drift effects from the IMU. In fact, with a careful setup in the beginning, it is possible to place the augmented marker on the acetabular fragment in a way such that it lies within the FOV at all times, reducing the influence of the drift error from the IMU even further.

#### V. CONCLUSION

We successfully demonstrated the feasibility of our augmented marker-based navigation system for PAO. The system is able to accurately track the acetabular orientation during the reorientation procedure.

#### REFERENCES

- [1] Behrens, A., Grimm, J.: Inertial navigation system for bladder endoscopy. 2011 Annual International Conference of the IEEE Engineering in Medicine and Biology Society pp. 5376–5379 (2011)
- [2] Beller, S., Eulenstein, S.: Upgrade of an optical navigation system with a permanent electromagnetic position control. Journal of Hepatobiliary Pancreat Surg 16(2), 165–70 (2009)
- [3] Claasen, G., Martin, P., Picard, F.: High-bandwidth low-latency tracking using optical and inertial sensors. Automation, Robotics and Applications (ICARA), 2011 5th International Conference on pp. 366–371 (2011)
- [4] Garrido-Jurado, S., Munoz-Salinas, R., Madrid-Cuevas, F.J., Marin-Jimenez, M.J.: Automatic generation and detection of highly reliable fiducial markers under occlusion. Pattern Recognition 47(6), 2280–2292 (2014)
- [5] Haid, M., Kamil, M., Chobtrong, T., Guenes, E.: Machine-vision-based and inertial-sensor-supported navigation system for minimal invasive surgery. AMA conferences 2013 - Sensor 2013 (2013)
- [6] Hsieh, P., Chang, Y., Shih, C.: Image-guided periacetabular osteotomy: computer-assisted navigation compared with the conventional technique: a randomized study of 36 patients followed for 2. Acta orthopaedica (2006)
- [7] Jaeger, M., Westhoff, B., Wild, A., Krauspe, R.: Computer-assisted Periacetabular Triple Osteotomy for Treatment of Dysplasia of the Hip. Zeitschrift fuer Orthopaedie und Ihre Grenzgebiete 142(1), 51–9 (2004)
- [8] von Jako, R.A., Carrino, J.A., Yonemura, K.S., Noda, G.A., Zhue, W., Blaskiewicz, D., Rajue, M., Groszmann, D.E., Weber, G.: Electromagnetic navigation for percutaneous guide-wire insertion: Accuracy and efficiency compared to conventional fluoroscopic guidance. NeuroImage 47(SUPPL. 2), 127–132 (2009)
- [9] Kalman, R.: A new approach to linear filtering and prediction problems. Journal of Fluids Engineering (1960)
- [10] Kim, S.J., Jeong, M.H., Lee, J.J., Lee, J.Y., Kim, K.G., You, B.J., Oh, S.R.: Robot head-eye calibration using the minimum variance method. In: 2010 IEEE International Conference on Robotics and Biomimetics, ROBIO 2010. pp. 1446–1451 (2010)
- [11] Langlotz, F., Stucki, M.: The first twelve cases of computer assisted periacetabular osteotomy. Computer Aided Surgery 2(6), 317–26 (1997)
- [12] Liu, L., Ecker, T., Schumann, S.: Computer assisted planning and navigation of periacetabular osteotomy with range of motion optimization. Medical Image Computing and Computer-Assisted Intervention MICCAI 2014 8674, 643–650 (2014)
- [13] Mahfouz, M., Kuhn, M.: Integration of UWB and wireless pressure mapping in surgical navigation. IEEE Transactions on Microwave Theory and Techniques 57(10), 2550–2564 (2009)
- [14] Murray, D.: The definition and measurement of acetabular orientation. Journal of Bone & Joint Surgery, British Volume (1993)
- [15] O'Donovan, K., Kamnik, R.: An inertial and magnetic sensor based technique for joint angle measurement. Journal of biomechanics (2007)
- [16] Park, F.C., Martin, B.J.: Robot Sensor Calibration: Solving  $AX = XB$  on the Euclidean Group. IEEE Transactions on Robotics and Automation 10(5), 717–721 (1994)
- [17] Pflugi, S., Liu, L., Ecker, T., Cullmann, J., Siebenrock, K., Zheng, G.: A cost-effective surgical navigation solution for periacetabular osteotomy (PAO) surgery. Computational Radiology for Orthopaedic Interventions pp. 333–348 (2016)
- [18] Pflugi, S., Vasireddy, R., Ecker, T., Lerch, T., Siebenrock, K., Zheng, G.: A Cost-Effective Navigation System for Peri-acetabular Osteotomy Surgery. MIAR 2016, Lecture Notes in Computer Science pp. 84–95 (2016)
- [19] Rambach, J.R., Teqari, A., Pagani, A., Stricker, D.: Learning to Fuse : A Deep Learning Approach to Visual-Inertial Camera Pose Estimation. IEEE Int Symp On Mixed and Augmented Reality (ISMAR) pp. 71–76 (2016)
- [20] Ren, H., Kazanzides, P.: Investigation of attitude tracking using an integrated inertial and magnetic navigation system for hand-held surgical instruments. IEEE/ASME Transactions on Mechatronics 17(2), 210–217 (2012)
- [21] Schweighofer, G., Pinz, A.: Robust pose estimation from a planar target. IEEE Transactions on Pattern Analysis and Machine Intelligence 28(12), 2024–2030 (2006)
- [22] Zhang, H., Banovac, F., Lin, R.: Electromagnetic tracking for abdominal interventions in computer aided surgery. Computer Aided Surgery 11(3), 127–36 (2006)